Biomaterials 29 (2008) 2637–2645

Contents lists available at ScienceDirect

Biomaterials

journal homepage: www.elsevier.com/locate/biomaterials

Bioadhesive hydrogel microenvironments to modulate epithelial morphogenesis

I-Ming Chung [a], Nduka O. Enemchukwu [b,c], Sirajud D. Khaja [c,d], Niren Murthy [c,d], Athanasios Mantalaris [a], Andrés J. García [b,c,*]

[a] Biological Systems Engineering Laboratory, Department of Chemical Engineering, Imperial College London, South Kensington campus, London SW7 2AZ, United Kingdom
[b] Woodruff School of Mechanical Engineering, Georgia Institute of Technology, 315 Ferst Drive, Atlanta, GA 30332-0363, USA
[c] Petit Institute for Bioengineering and Bioscience, Georgia Institute of Technology, 315 Ferst Drive, Atlanta, GA 30332-0363, USA
[d] Coulter Department of Biomedical Engineering, Georgia Institute of Technology, 315 Ferst Drive, Atlanta, GA 30332-0363, USA

ARTICLE INFO

Article history:
Received 18 January 2008
Accepted 13 March 2008
Available online 30 March 2008

Keywords:
Cell adhesion
Extracellular matrix
Differentiation
Laminin
RGD

ABSTRACT

Epithelial cells polarize and differentiate into organotypic cell aggregates in response to cell–cell and cell–matrix interactions. For example, Madin–Darby Canine Kidney (MDCK) cells form spherical cell aggregates (cysts) with distinct apical and basolateral polarity when cultured three dimensionally (embedded) in type I collagen gels. To investigate the effects of individual extracellular factors on epithelial morphogenesis, we engineered fast degrading protease-responsive polyethylene glycol (PEG) hydrogels functionalized with controlled densities of various bioligands (RGD peptide, laminin-1 (LN)) to allow 3D culturing of MDCK cells, cyst expansion, and morphogenesis/polarization. Cysts formed after 15 days of culture in these hydrogels were analyzed with multiphoton fluorescence microscopy for markers of apical and basolateral membrane domains. Epithelial cysts formed in bioadhesive ligand-functionalized PEG gels exhibited a higher frequency of central lumen and interior apical pole formation as well as basolateral polarization compared to those of unmodified PEG hydrogels. These results demonstrate that incorporation of specific bioadhesive motifs into synthetic hydrogels provides 3D culture environments that support epithelial morphogenesis. These microenvironments provide a flexible and controlled system for systematic investigations into normal and pathologic morphogenic behaviours as well as synthetic environments for promoting tissue morphogenesis for regenerative medicine applications.

1. Introduction

Epithelial morphogenesis plays a central role in developmental biology by directing the organization of tissues and organs as well as producing the diversity of body shapes found in multicellular organisms [1]. Epithelial morphogenesis is a highly complex multistep process that requires coordinated cell–cell and cell–extracellular matrix (ECM) interactions [2–7] and cellular behaviours over space and time to create functional 3D structures [1,8,9]. First, patterns of different cell populations undergoing particular morphogenetic movements are established by a group of genes that control germ layer fates [10]. Second, cell–cell and cell–matrix interactions activate epithelial morphogenetic events and generate cell polarity through the reorganization of proteins in the cytoplasm and on the plasma membrane [11–13]. Finally, a combination of cellular processes including proliferation, adhesion, migration and apoptosis contributes to the eventual epithelial tissue architecture [4,9,14,15].

Epithelia are coherent sheets of cells that cover the external surface of the body and line all its internal cavities [16,17]. Most internal epithelial organs consist of monolayers of cells that adhere to each other through cell–cell junctions. These monolayers are arranged in spherical (cysts) or tubular (tubules) structures that enclose a central lumen and are surrounded by a basement membrane [9]. The key functions of epithelia are to control tissue architecture, create impervious and selective permeability fluid barriers between biological compartments, and perform vectorial transport functions (for example, absorption, secretion, ion transport and transcytosis) which are crucial for the survival of multicellular organisms [17–19]. In order to carry out these specialized tasks, epithelial cells must polarize internally to create biochemically different surfaces by segregating their plasma membrane proteins into apical (facing lumen), lateral (facing neighbouring cells) and basal (facing the underlying ECM) domains [20]. Since many proteins (such as β-catenin) localize to both the basal and lateral domains, these domains are often collectively referred to as 'basolateral' [9].

* Corresponding author. Woodruff School of Mechanical Engineering, Georgia Institute of Technology, 315 Ferst Drive, 2314 IBB Atlanta, GA 30332-0363, USA. Tel.: +1 404 894 9384; fax: +1 404 385 1397.
E-mail address: andres.garcia@me.gatech.edu (A.J. García).

0142-9612/$ – see front matter © 2008 Elsevier Ltd. All rights reserved.
doi:10.1016/j.biomaterials.2008.03.008

Bissell and colleagues have pioneered the use of 3D collagen gels to study how ECM microenvironments regulate epithelial morphogenesis and functions since the early 1980s [21–24]. It is well established that many epithelial cells, including Madin–Darby Canine Kidney (MDCK) cells, form tissue-like cysts with classical apical and basolateral polarity when cultured three dimensionally (embedded) in type I collagen gels [8,9,24]. The organization of these cysts closely resembles that of epithelia *in vivo*, and thus cyst development provides an ideal model system for the formation of a rudimentary epithelial suborgan [22]. Recent studies in epithelial developmental systems have demonstrated the important roles of cell–cell and cell–ECM interactions in the establishment of cell polarity, while the ECM has been implicated as a potential link between polarity and tissue organization [4,21,22,24–28]. For example, when MDCK cells are grown in suspension culture (i.e. without exogenous ECM), they will attempt to compensate for the lack of ECM in their culture environment by creating internal cavities and filling them with secreted basement membrane to generate basal surfaces *de novo*, resulting in the formation of hollow cysts with opposite polarity (apical surface on the outside, basolateral surface on the inside) compared to the collagen gel-grown cysts [8].

To date, most epithelial morphogenesis studies have been cell-based (i.e. utilizing genetic modification techniques to control cellular expressions and investigate the resultant effects), while the 3D culture environments employed have always been limited to collagen gels [8,17,26,28]. Although collagen gels are part of the components of the natural ECM, they do not provide controlled presentation of specific bioligands or degradation motifs, making it difficult to isolate the effects of a specific bioligand of interest on the epithelial morphogenetic behaviour. As such, no studies have yet been carried out to systematically investigate the effects of individual extracellular factors on epithelial morphogenesis largely due to the lack of suitable ECM mimetics for this kind of work. Furthermore, the construction of *in vitro* cell culture systems that reconstitute the 3D polarized organization and structure of native tissues and organs constitutes a major challenge in tissue engineering and regenerative medicine applications.

To this end, we have engineered biomimetic hydrogels incorporating tethered bioligands to provide signals for modulating morphogenesis and crosslinkers with protease-sensitive degradation sites to allow cells to proteolytically create space to expand inside the gel and form cysts. Specifically, PEG was selected as the inert main structural component due to its well-established cytocompatibility and resistance to protein adsorption [29,30], allowing only the biological signal from the incorporated peptides or proteins to be exhibited to the surrounding cells with minimal biochemical background. These synthetic hydrogels were originally developed by Hubbell and colleagues and have recently been successfully employed as an alternative ECM model for guiding cellular behaviour in 3D cell migration research [31–35]. The hydrogels are based on end-functionalized 4-arm PEG macromers, reacted via Michael-type addition reaction with cysteine-containing peptides or proteins, then crosslinked with bis-cysteine oligopeptides under near physiological conditions in the presence of cells, resulting in a 3D hybrid network that encapsulates cells. In the present study, we examined the suitability of proteolytically degradable PEG hydrogels functionalized with bioadhesive ligands as a bioartificial ECM model system for investigating and directing epithelial morphogenesis.

2. Materials and methods

2.1. Cell culture

MDCK cells (NBL-2; ATCC, Manassas, VA) were maintained in Eagle's minimal essential medium with Earle's BSS (EMEM; ATCC, Manassas, VA) supplemented with 10% FBS, 100 U/ml penicillin, and 100 μg/ml streptomycin (Invitrogen, Carlsbad, CA) in 5% CO_2, 95% air at 37 °C. Cells were enzymatically detached from culture dishes using 0.05% trypsin/0.02% EDTA (Invitrogen), centrifuged at 400 × g for 5 min, and resuspended in culture medium.

2.2. MDCK cell encapsulation and 3D culture in collagen gels

3D cyst culture in collagen gels was carried out as described previously [26,27]. Prior to MDCK cell preparation, type I collagen solution containing 66% Vitrogen (3 mg/ml; Cohesion Technologies, Palo Alto, CA), 12% 200 mM glutamine, 10% 10× MEM (Sigma–Aldrich, Saint Louis, MO), 2% 1.0 M HEPES (pH 7.6), and 10% 23.5 mg/ml $NaHCO_3$ in dH_2O was gently mixed at 4 °C. MDCK cells grown on culture dishes were then trypsinized, pelleted, and resuspended at room temperature into a dispersed single-cell suspension (2×10^4 cells/ml) in the type I collagen solution. This cell–collagen mixture was then cast onto Nunc Anopore membrane filter inserts (10 mm diameter, 0.2 μm pore size; Fisher Scientific, Pittsburgh, PA) at 150 μl per insert, and allowed to gel in a 37 °C oven (100% air) for 20 min. After gelling, inserts were placed in 24-well plate, 0.5 ml of culture medium was added to both the top and bottom of each gel, and incubated at 37 °C, 95% air, 5% CO_2. Cultures were fed every 2–3 days and grown for 12 days until cysts with lumens were formed.

2.3. Synthesis of PEG–VS

Branched 4-arm PEGs (Sunbright PTE-20000, MW = 19 858; NEKTAR Therapeutics, San Carlos, CA) were functionalized at the OH-termini with divinyl sulfone (Sigma–Aldrich) as described previously [31]. In brief, PEG–VS was synthesized by reacting a dichloromethane solution of the PEG–OH (previously dried over molecular sieves) with NaH under argon gas and then, after hydrogen evolution, with diVS (molar ratios: OH 1/NaH 5/diVS 50), at room temperature for 3 days, under argon gas with stirring. The resulting solution was subsequently neutralized with 99.8% acetic acid and filtered through a filter paper until clear. This VS-functionalized PEG was then precipitated in ice cold diethyl ether, washed, and re-dissolved in dichloromethane; this cycle was repeated twice to remove all excess diVS, and PEG–VS was finally dried under vacuum. The success of VS conversion on the OH-termini was confirmed by ^{1}H NMR spectroscopy with characteristic peaks at 6.1, 6.4 and 6.8 ppm, while the degree of conversion was found to be 90–95%.

2.4. PEG gel preparation and 2D/3D culture of MDCK cells

Mono-cysteine RGD peptide and laminin protein containing cysteine groups were employed to enable bioligand tethering onto PEG–VS. The integrin-binding peptide with RGD (Arg-Gly-Asp) motif Ac-*GRGD*SPC–NH_2 was synthesized and HPLC purified by Emory University Microchemical Facility (Atlanta, GA), while mouse laminin-1 (LN, 1.3 mg/ml, isolated from the Engelbreth–Holm–Swarm (EHS) sarcoma) was obtained from Invitrogen (Carlsbad, CA). To prepare bioligand-tethered PEG gels for 3D cell encapsulation, the 4-arm PEG–VS powder was first dissolved in triethanolamine (TEOA, 0.3 M, pH 8) buffer to give a 10% (w/v) solution, then various amounts of the RGD peptide or LN protein (in TEOA, 0.3 M, pH 8) was added to this solution and allowed to react for 30 min at 37 °C. Next, the culture medium containing dispersed single cells (1×10^6 cells/ml after crosslinking) and the fast degrading MMP-sensitive bis-cysteine crosslinker peptide (Ac-GCRD–GPQG ↓ IWGQ–DRCG–NH_2, ↓ indicates the cleavage site; HPLC purified, Emory University Microchemical Facility) dissolved in TEOA buffer (0.3 M, pH 10) was added to the PEG solution and gently mixed. This cell–PEG mixture was then quickly cast onto Nunc Anopore membrane filter inserts (10 mm diameter, 0.2 μm pore size; Fisher Scientific, Pittsburgh, PA) at 50 μl per insert, and allowed to crosslink and solidify by incubating at 37 °C for 15 min. After gelling, inserts were placed in 24-well plate, 0.5 ml of culture medium was added to both the top and bottom of each gel, and plates were incubated at 37 °C, 95% air, 5% CO_2. Cultures were fed every 2–3 days and grown for 15 days before harvest. A much higher cell seeding density (1×10^6 cells/ml) was employed for 3D PEG hydrogel cultures (compared to 2×10^4 cells/ml in collagen gel cultures) to ensure that adequate amount of MMPs could be secreted by the MDCK cells to effectively break through the PEG gel network, thereby creating necessary spaces for the cells to proliferate and form cysts. For non-degradable, MMP-insensitive PEG gels, the crosslinker was switched to 3,6-dioxa-1,8-octane-dithiol (DODT; Sigma–Aldrich).

For 2D MDCK culture on top of PEG gels, the gel preparation steps were similar to the above-mentioned 3D culture, except that instead of adding the cells together with the crosslinker to the PEG solution, the cells were only seeded (5×10^3 cells/cm^2) onto the non-degradable DODT-crosslinked PEG gels after the gels had solidified.

For both 3D and 2D cultures, each PEG hydrogel employed was 50 μl in final volume, and consisted of 20 μl PEG–VS solution (5.0 mg, 1.0×10^{-6} mol of VS groups), 10 μl RGD peptide or LN protein solution with desired concentrations (to ensure that bioligand-functionalized PEGs still possessed Michael-type reactivity for later crosslinking, the molar ratio of bioligand:VS should not exceed 1:20), 10 μl cell suspension (5.0×10^4 cells) or 10 μl PBS without cells in the case of 2D cell culture, and 10 μl crosslinker solution (5.0×10^{-7} mol; molar ratio of crosslinker:VS = 1:2). It should be noted that while the volume of MMP-insensitive PEG gels remained constant over the 15 days 3D MDCK culturing period, in the case of MMP-sensitive

PEG hydrogels, the gel volume swelled from the initial gel thickness of around 0.64 mm (50 μl) at the beginning of the 3D MDCK culture to an eventual gel thickness of around 1.5 mm after 15 days culture. The observed swelling of these hydrogels is a result of passive swelling and degradation of the PEG gel network by MMPs secreted from the growing MDCK cells. This swelling behaviour of MMP-sensitive PEG hydrogels was also reported by Hubbell and colleagues [31].

2.5. Immunofluorescence (IF) staining

The primary antibody used in this study was rabbit anti-β-catenin (Santa Cruz Biotechnology, Santa Cruz, CA). Secondary antibody used was goat anti-rabbit Alexa Fluor 488 (Molecular Probes, Eugene, OR). Actin filaments were stained with rhodamine phalloidin (Invitrogen, Carlsbad, CA), and nuclei were stained with Hoechst 33342 (Invitrogen).

For cysts cultured in type I collagen gels, the IF staining procedure was carried out as described previously [27]. Samples were first washed with PBS+ (PBS containing Ca^{2+} and Mg^{2+}), then treated with collagenase type VII (diluted to 100 U/ml in PBS+; Sigma–Aldrich) at 37 °C for 10 min to increase epitope accessibility. This step was followed by fixation with 4% paraformaldehyde (in PBS+) for 30 min and quenching with 75 mM NH_4Cl and 20 mM glycine in PBS+ for 10 min. All steps were carried out at room temperature unless stated otherwise, and between each step, the samples were extensively washed with PBS+ (3× rinses and 2 × 5 min, with gentle rocking). Next, samples were permeabilized and blocked with blocking buffer containing 0.025% saponin (Calbiochem, San Diego, CA), 0.7% fish gelatin (Sigma–Aldrich) and 0.02% NaN_3 in PBS+ for 30 min. The samples were then incubated in diluted primary antibody (1:50) overnight, followed by an overnight incubation with diluted secondary antibody (1:200), rhodamine phalloidin (1:50), and Hoechst 33342 (1:5000) in blocking buffer. The antibody incubation steps were carried out at room temperature with extensive blocking buffer washing (1× rinse, 3 × 10 min, with gentle rocking) after each step. Samples were then postfixed with 4% paraformaldehyde for 30 min and washed with PBS+. After adding a drop of Biomeda Gel/Mount (Electron Microscopy Sciences, Hatfield, PA) to each sample, the collagen gel was punched out of the filter insert and carefully peeled away from the filter using forceps. Each gel was then placed on a microscope slide with the upside of the gel facing up (this facilitates confocal analysis), mounted with a drop of Biomeda Gel/Mount, covered with a glass coverslip, and allowed to harden overnight in the dark before sealing the edges of the coverslip with nail polish.

For cysts cultured in PEG gels, the IF staining procedure was similar to the one used for collagen gels, but with two modifications. First, since there was no collagen in our PEG gels, the PEG gels were not treated with collagenase before fixation. Second, unlike collagen gels which were very thin (~0.2 mm), the extracted PEG gels were much thicker (~1.5 mm), and could not be properly sealed by just adding a coverslip on top of a microscope slide. To circumvent this problem, before mounting, thick pre-cut silicone gaskets (1.5 mm thick) with six pre-cut circular holes (9 mm diameter; Grace Bio-Labs Inc., Bend, OR) were used as spacers, and glued onto the microscope slides; while the extracted PEG gels were cut into 6 mm diameter discs with a dermal biopsy punch (Miltex Inc., York, PA), and placed inside the holes of these silicone gaskets (now glued to the microscope slides). The gel samples were then mounted by adding enough Biomeda Gel/Mount to fill up the remaining space, and sealed in place by placing a coverslip on top of the silicone gasket. The mounted samples were then allowed to harden overnight in the dark before sealing the edges of the coverslip with nail polish.

2.6. Image analysis and quantification of cyst phenotypes

To quantify cyst phenotypes, cysts formed in gels were fixed and then immunofluorescently stained for β-catenin, actin, and nuclei as described above. The stained samples were then imaged with a Plan-Neofluor 40× 1.3 NA objective on a Zeiss LSM/NLO 510 multiphoton microscope. Digital images of optical sections at the mid-plane of cysts were collected in the *x*–*y* plane of the sample and analyzed using the Zeiss LSM5 Image Browser software.

Imaged cysts were classified as possessing an interior apical pole, a peripheral apical pole, an ambiguous apical pole and basolateral polarization on the basis of the following criteria: (i) cysts with intense actin staining at either an interior luminal surface or at cell–cell contacts were considered to possess an interior apical pole; (ii) cysts with intense actin staining at the cyst–substratum interface were considered to possess a peripheral apical pole; (iii) cysts that lacked intense actin staining/or cysts that exhibited actin staining both in the cyst interior and the cyst–substratum interface were considered to possess an ambiguous apical pole; and (iv) cysts with intense β-catenin staining at cell–cell contacts and basement membrane were considered to possess a basolateral polarization. The presence of a well-defined lumen, shape (spheroid or cluster), size (diameter) and the number of nuclei at the mid-plane cross-section of each cyst were also recorded. More than 30 cysts were analyzed for each condition in three independent experiments.

2.7. Statistical analysis

Comparisons of cyst phenotype parameters among all experimental conditions were carried out using the non-parametric Kruskal–Wallis ANOVA ($p < 0.05$ considered significant), followed by pair-wise comparison using two-Sample Mann–Whitney test with Bonferoni adjustment for parameters that were shown to be significant from the Kruskal–Wallis analysis. This Bonferoni adjustment involves dividing the alpha level of 0.05 by the number of tests that one intends to use and using the revised alpha level as the new criteria for determining significance ($p < 0.05/3$ tests $= 0.0167$, i.e. $p < 0.0167$ considered significant).

3. Results

3.1. 2D MDCK cell spreading on PEG hydrogels

We engineered proteolytically degradable PEG hydrogels functionalized with bioadhesive ligands as a bioartificial ECM model system for investigating and directing epithelial morphogenesis. We examined two bioadhesive ligands: (i) RGD, the minimal integrin receptor binding motif derived from fibronectin and other ECM proteins that is widely used to guide cellular adhesion and migration [31,32], and (ii) natural laminin-1 protein (LN), a major component of basement membrane implicated in MDCK cysts polarization [26,28]. To confirm successful grafting and bioactivity of bioadhesive ligands tethered onto the PEG chains, and to test whether the extent of 2D cell spreading on PEG hydrogels was dependent on the incorporated bioligand density, we cultured MDCK cells on top of unmodified PEG hydrogels and hydrogels grafted with various densities (0.01, 0.1 and 1.0 mM) of RGD peptides. All PEG hydrogels used in 2D culture experiments were crosslinked with non-degradable DODT crosslinkers to prevent gel degradation and to provide secure anchoring for tethered RGD peptides. MDCK cells were seeded onto the hydrogels at 5×10^3 cells/cm^2 and the extent of cell spreading was determined at 3, 30 and 70 h post-seeding.

Light microscopic images (Fig. 1A, C) revealed that, as expected, there was no cell spreading on unmodified PEG hydrogels even at 70 h after seeding due to PEG's resistance to protein adsorption and non-specific cell adhesion. In the case of RGD-grafted PEG gels, cell spreading was observed as early as 3 h post-seeding on 1.0 mM RGD–PEG gels (Fig. 1J), and was apparent on all densities of RGD at 30 h after seeding (Fig. 1E, H, and K). It was also evident that the extent of cell spreading increased both with time and increasing density of grafted RGD peptide, with 1.0 mM RGD–PEG gels showing the greatest extent of cell spreading at 70 h after seeding (Fig. 1L), confirming successful grafting and bioactivity of controlled densities of bioligands onto PEG gels.

3.2. 3D MDCK culture in type I collagen gels

It is well established that when MDCK cells are cultured three dimensionally in type I collagen gels, they form polarized cysts with an apical domain that faces the central lumen and a basolateral domain that faces the neighbouring cells and ECM [8,9]. Therefore, 3D MDCK collagen gel cultures were carried out to serve as a reference control condition for comparing with other 3D MDCK PEG gel culture experiments.

MDCK cells were embedded in type I collagen gels with a seeding density of 2×10^4 cells/ml gel, and allowed to grow for 12 days before harvest. Consistent with previous studies [26,27], each cyst arose from the proliferation of a single MDCK cell; generally, cysts started forming lumens around day 4, and matured by 12 days. To characterize polarization, cysts formed in gels were fixed and immunostained for actin (apical marker; actin is enriched in apical microvilli), β-catenin (an intracellular cytoskeletal protein localized to adherens junctions) and cell nuclei. These stained cysts were then scanned with a multiphoton fluorescence microscope at the mid-plane of the cysts. A typical multiphoton optical sectioning of a cyst formed in type I collagen gel (Fig. 2) showed a spherical monolayer of polarized cells that enclosed a central lumen, with clearly defined nuclei (blue), lumen-facing apical domain (red) and

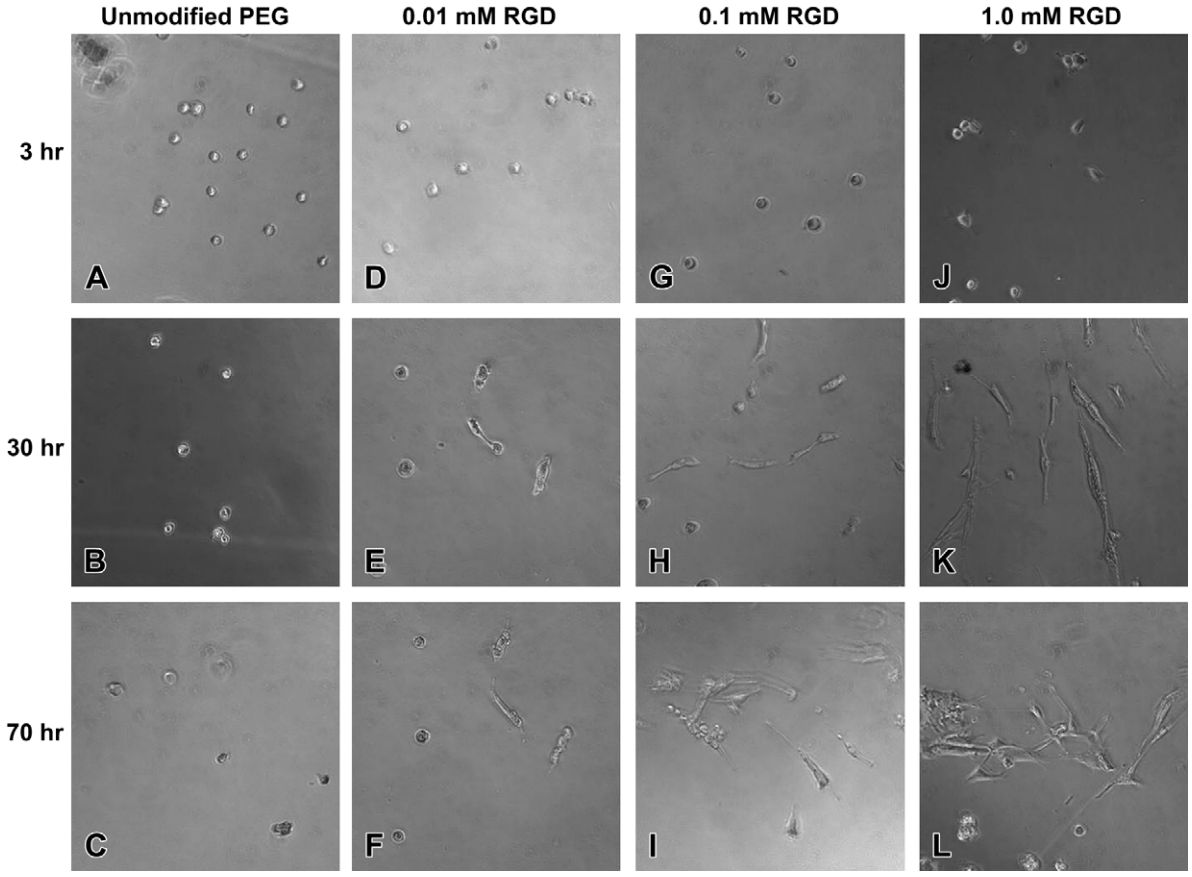

Fig. 1. Light microscopy (200× magnification) of 2D MDCK cultures on unmodified PEG hydrogels and PEG hydrogels grafted with various densities (0.01, 0.1 and 1.0 mM) of RGD peptides taken at 3, 30 and 70 h post-seeding.

basolateral domain (green). These staining patterns are in excellent agreement with previous studies [9,26,28].

3.3. 3D MDCK culture in PEG hydrogels

To evaluate the effects of our engineered PEG hydrogels on the morphogenesis and polarization of MDCK cysts, 3D cultures of MDCK cells were carried out within unmodified PEG hydrogels and PEG hydrogels grafted with 1.0 mM RGD peptide or 100 μg/ml LN. All PEG hydrogels used in 3D culture experiments were crosslinked with fast degrading MMP-sensitive bis-cysteine oligopeptides to allow cells to proteolytically create necessary space inside the gels during proliferation and cyst formation. The utilization of degradable MMP-sensitive crosslinker was essential for cyst development in our PEG hydrogels since the mesh size of the PEG hydrogels is too small (only about 30–50 nm as calculated from the swelling obtained by classic Flory–Rehner analysis [31,36], which is two orders of magnitude smaller than the size of MDCK cells) to allow any cell proliferation or cyst formation. Indeed, when we cultured MDCK cells three dimensionally in various PEG gels crosslinked with non-degradable DODT crosslinkers, the cells remained rounded and did not proliferate even after 3 weeks, although cell viability remained high (~80%).

MDCK cells, dispersed into single cells, were embedded within MMP-degradable PEG hydrogels and cultured for 15 days before harvest. Light microscopic images (Fig. 3A–F) taken at days 7 and 12 of culture showed that both the number and the size of cysts increased with time in all conditions. It is worth noting that in the

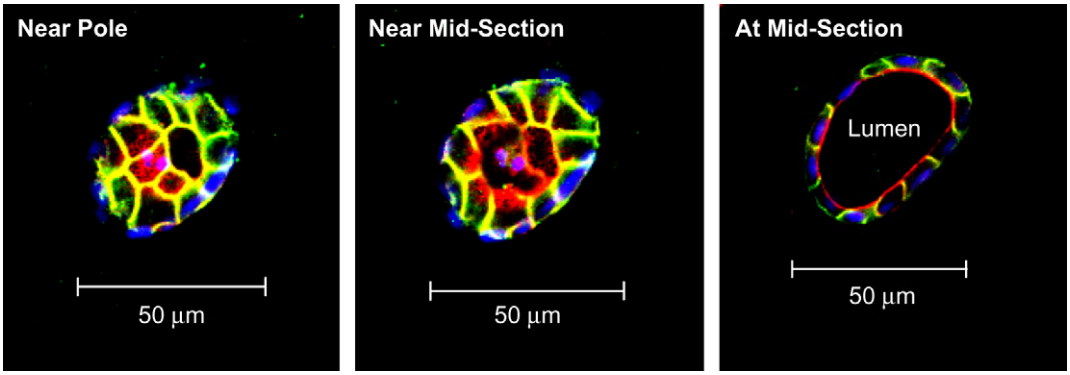

Fig. 2. Serial multiphoton optical sections (at 4 μm intervals) through an MDCK cyst cultured in type I collagen gel. The apical domain (red) is stained for actin, which is enriched in luminal microvilli. The basolateral domain (green) is stained for β-catenin, which is localized in the adherens junctions. The nuclei (blue) are stained with Hoechst dye.

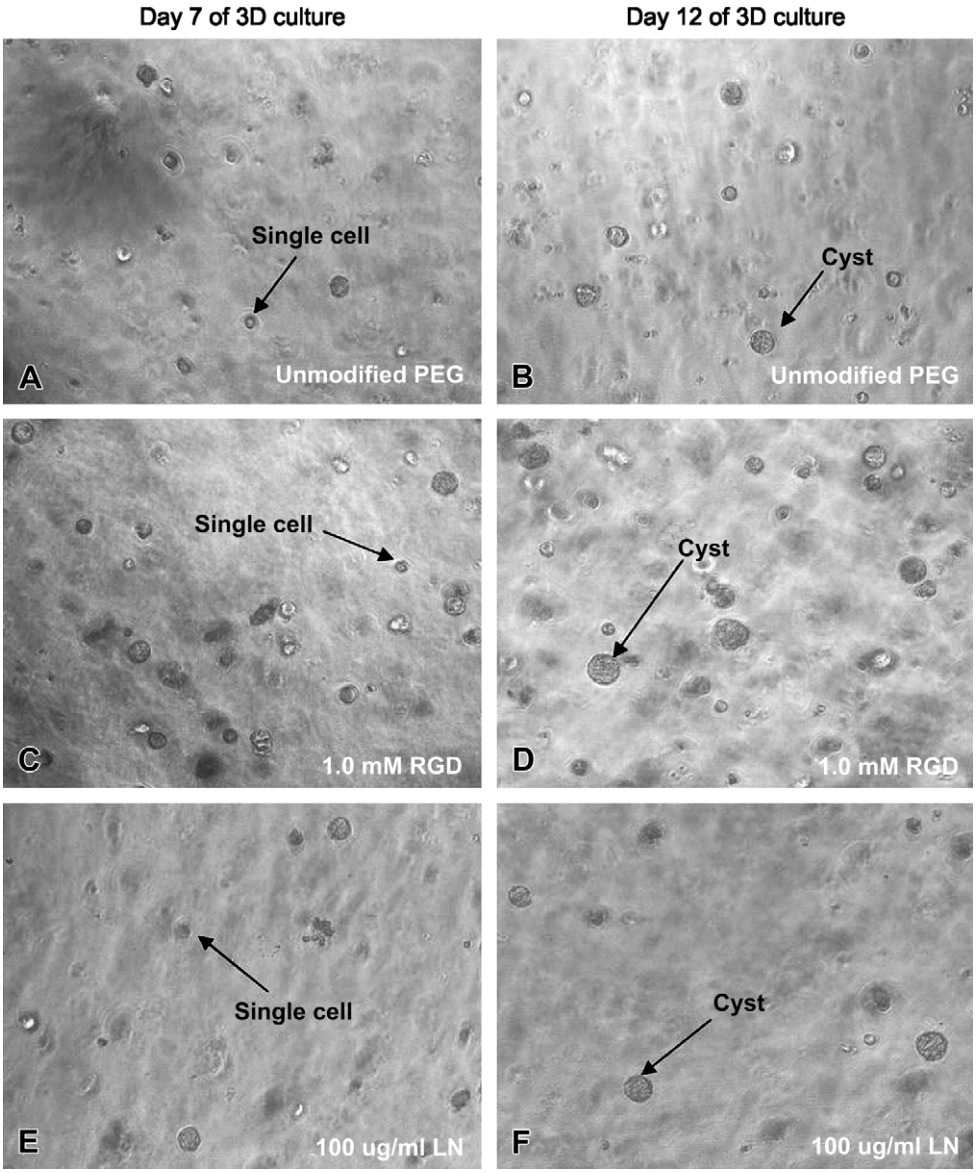

Fig. 3. Light microscopy (100× magnification) of 3D MDCK cultures in unmodified PEG hydrogels and PEG hydrogels grafted with 1.0 mM RGD peptides and 100 μg/ml LN, taken at 7 and 12 days post-seeding. Both the number and the size of cysts increased with time in all samples. It is worth noting that in the 1.0 mM RGD–PEG gel, the cysts seemed to be larger and more in number compared to those in other gels.

1.0 mM RGD–PEG gel, the cysts were larger and more in number compared to those in other gels. These light microscopic observations were further confirmed by the quantitative and statistical analyses of the multiphoton microscopic images of the cysts cultured in PEG hydrogels which are presented in Tables 1, 2. Cysts formed in PEG hydrogels were fixed, immunostained and then imaged under a multiphoton fluorescence microscope. In order to quantify and compare cyst phenotype for morphogenesis evaluation, multiphoton imaged cysts were classified as possessing an interior apical pole, a peripheral apical pole, an ambiguous apical pole or basolateral polarization on the basis of the following criteria: cysts with intense actin staining (red) at either an interior luminal surface or at cell–cell contacts were considered to possess an interior apical pole (Fig. 4A); cysts with intense actin staining at the cyst–substratum interface were considered to possess a peripheral apical pole (Fig. 4B); cysts that lacked intense actin staining or cysts that exhibited actin staining both in the cyst interior and the cyst–substratum interface were considered to possess an ambiguous apical pole (Fig. 4C); cysts with intense β-catenin staining (green) at cell–cell contacts and basement membrane were

Table 1
Cyst phenotypes for MDCK cysts harvested from 15-day 3D cultures in unmodified PEG hydrogels and PEG hydrogels grafted with 1.0 mM RGD or 100 μg/ml LN

Parameters	Unmodified PEG	100 μg/ml LN–PEG	1.0 mM RGD–PEG	Kruskal–Wallis test for three groups
Size (μm)	39 ± 9.7	35.0 ± 6.5	46.8 ± 10.6	*S*
Number of nuclei	7.8 ± 2.9	6.0 ± 2.0	9.7 ± 3.3	*S*
Aggregate type (spheroid)	*0.87*	*0.88*	*0.91*	NS
Aggregate type (cluster)	*0.13*	*0.12*	*0.09*	NS
Presence of lumen	*0.17*	*0.40*	*0.54*	*S*
Interior apical polarization	*0.18*	*0.39*	*0.55*	*S*
Peripheral apical polarization	*0.13*	*0.08*	*0.02*	NS
Ambiguous apical polarization	*0.61*	*0.52*	*0.64*	NS
Basolateral polarization	*0.53*	*0.71*	*0.77*	*S*

Sample size (n) = 30 per condition. S = significant ($p < 0.05$); NS = not significant ($p > 0.05$). Scoring system was used to semi-quantify non-quantitative parameters (in italic), scores of 1.0 being the fullest extent, scores of 0 being the least extent.

Table 2
Pair-wise comparisons between different PEG hydrogels

Parameters	Unmodified PEG vs. LN	Unmodified PEG vs. RGD	LN vs. RGD
Size (μm)	NS	S	S
Number of nuclei	NS	NS	S
Presence of lumen	S	S	NS
Interior apical polarization	NS	S	NS
Basolateral polarization	NS	S	NS

S = significant ($p < 0.0167$); NS = not significant ($p > 0.0167$).

considered to possess a basolateral polarization (Fig. 4D). The extent of polarization for each of the above categories (interior, peripheral, ambiguous and basolateral) was semi-quantitatively analyzed using a scoring system with scores of 0, 0.5 and 1.0. Cysts with scores of 1.0 for each interior apical polarization and basolateral polarization represent structures with the closest resemblance to the phenotypes of classical MDCK cysts grown in type I collagen gel; whereas scores of 0 represent the opposite. We note that the parameter "peripheral apical polarization" refers to the phenotype of abnormal cysts. The shape (spheroid or cluster), size (diameter) and the number of nuclei at the mid-plane cross-section of each cyst were also recorded. These quantitative results were statistically analyzed, and are presented in Tables 1, 2 and Fig. 6. It is also worth noting that the total score of the three types of apical polarizations (interior, peripheral and ambiguous) for each cyst does not necessarily have to add up to 1.0. For example, in the case where a cyst has strong interior apical polarization but also some degree of peripheral apical polarization (such as in Fig. 5F), the cyst will have a score of 1.0 for the interior apical polarization, a score of 0.5 for the ambiguous apical polarization (for having a combination of interior and peripheral polarization), and a score of 0 for the peripheral polarization. On the other hand, for a cyst that only exhibits partial interior apical polarization but no peripheral apical polarization, it would have a score of 0.5 for the interior apical polarization, a score of 0 for peripheral apical polarization, and a score of 0 for ambiguous apical polarization, which would result in a total apical polarization score of 0.5 for this cyst.

Multiphoton fluorescence microscopic images (Fig. 5A–F) of cysts grown in all three types of PEG gels revealed that MDCK cysts formed in PEG gels functionalized with either LN (Fig. 5C, D) or RGD (Fig. 5F) generally exhibited cyst phenotypes more akin to the classical cysts formed in collagen gels (Fig. 2), with a well-defined lumen and normal polarization (i.e. apical surface bordering the lumen on the inside, basolateral surface on the outside and at cell–cell contacts). In contrast, MDCK cysts grown in unmodified PEG gels (Fig. 5A, B) displayed a higher frequency of inverted polarization (i.e. apical surface on the outside, basolateral surface on the inside) with a less defined lumen, which were quite similar to the abnormal cysts observed in suspension cultures. Furthermore, cysts grown in RGD–PEG gels (Figs. 5E, F and 3C, D) were significantly larger in size than those from the other two PEG gels. Indeed, quantitative analyses (Tables 1, 2, and Fig. 6) of cyst phenotypes for MDCK cultures in these three types of PEG gels showed significant differences among them in terms of size, number of nuclei, presence of lumen, interior apical polarization and basolateral polarization; with cysts from the RGD–PEG gels having the highest score matching the phenotypes of a classical cyst, followed by LN–PEG gels, and finally, unmodified PEG gels.

4. Discussion

3D culture systems provide a unique platform for the study of cell signalling and cell–matrix interactions in a more *in vivo* like environment than 2D culture [32,37,38]. As such, 3D culture systems have now become an indispensable tool for investigating the molecular signals that specify epithelial architecture [9,26,28]. In this work, we introduced fast degrading protease-sensitive PEG hydrogels functionalized with controlled densities of bioligands as a surrogate ECM model system to study the effects of individual extracellular factors on epithelial morphogenesis. Our engineered bioartificial 3D culture system is better suited for this particular task than conventional collagen gel because the main structural PEG component is resistant to protein adsorption [29,30], enabling only the biological signal from the incorporated peptide or protein to be exhibited to the surrounding cells with minimal biochemical background, therefore allowing a more rigorous investigation of the effects of individual bioligands. In addition, this synthetic matrix provides the controlled presentation of specific bioactive motifs, such as bioadhesive ligands and protease-sensitive sequences.

2D cell culture experiments on unmodified PEG gels and gels functionalized with varying RGD densities clearly demonstrated that while no cell spreading was observed on the unmodified PEG gels, the extent of cell spreading on the RGD-functionalized PEG gels was regulated by increasing the densities of incorporated peptides. These findings confirm the non-adhesive nature of the bare PEG gels [37] and the successful incorporation of controlled densities and biological availability of bioligands into the otherwise inert PEG networks. This observation also indicates that the cellular responses to the bioligand-functionalized PEG gels will be mostly, if not solely, due to the incorporated bioligands.

It is widely accepted that epithelial morphogenesis requires the dynamic interactions of the epithelial cells with ECM, and the key molecules involved in these interactions are the integrin family of cell surface ECM receptors. Previous studies have indicated that

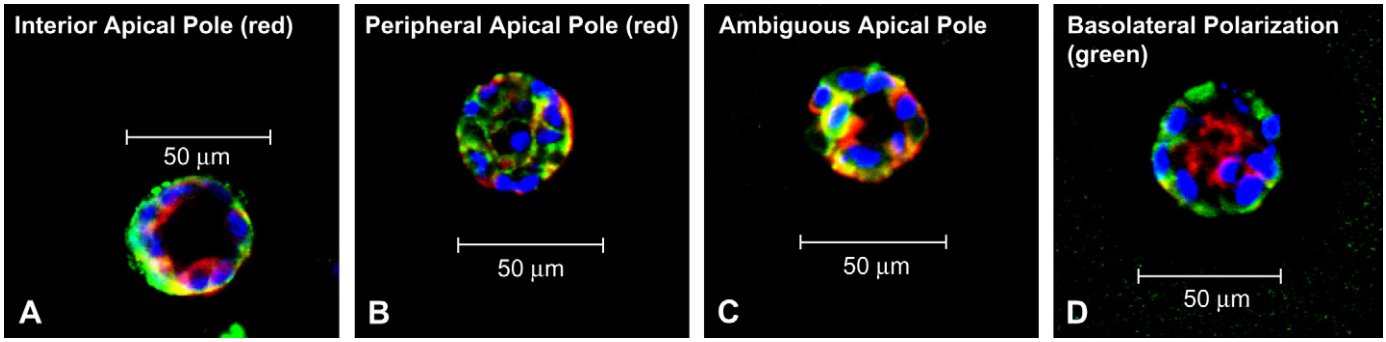

Fig. 4. Multiphoton fluorescence microscopic images of MDCK cysts cultured in PEG hydrogels, showing various types of apical and basolateral polarization for cyst phenotype classification: (A) cysts with intense actin staining (red) at either an interior luminal surface or at cell–cell contacts were considered to possess an interior apical pole; (B) cysts with intense actin staining at the cyst–substratum interface were considered to possess a peripheral apical pole; (C) cysts that lacked intense actin staining or cysts that exhibited actin staining both in the cyst interior and the cyst–substratum interface were considered to possess an ambiguous apical pole; (D) cysts with intense β-catenin staining (green) at cell–cell contacts and basement membrane were considered to possess a basolateral polarization.

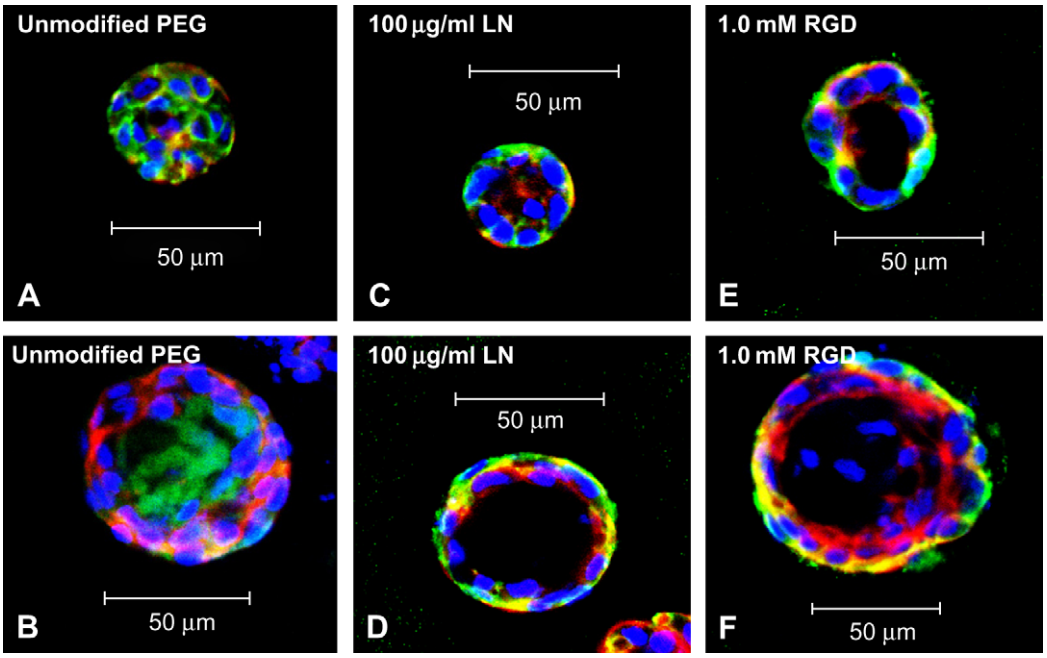

Fig. 5. Typical multiphoton fluorescence microscopic images of MDCK cysts cultured for 15 days in (A, B) unmodified PEG hydrogels, (C, D) PEG hydrogels with 100 μg/ml LN, and (E, F) PEG hydrogels with 1.0 mM RGD. Apical markers were stained red, basolateral markers green, and nuclei blue. Cysts formed in unmodified PEG hydrogels were much less likely to have a central lumen, interior apical pole, and basolateral polarization compared to those formed in bioligand-functionalised PEG gels.

both β_1 integrin and extracellular laminin play vital roles in the orientation of epithelial cyst polarity as well as in the maintenance of epithelial structure and function [28,39]. To modulate epithelial morphogenesis and investigate the effects of individual extracellular factors on the MDCK cyst phenotype, we selected RGD peptide and laminin as the functional extracellular bioligands to be incorporated into the proteolytically degradable PEG gels.

PEG hydrogels presenting bioadhesive RGD and LN ligands promoted epithelial morphogenesis to a larger extent than the unmodified gels. Indeed, these engineered hydrogels supported the expression of differentiation/polarization markers to a similar extent than the natural matrix type I collagen. Taken together, these results indicate that the presentation of integrin ligands on the PEG backbone promotes epithelial morphogenesis, consistent with

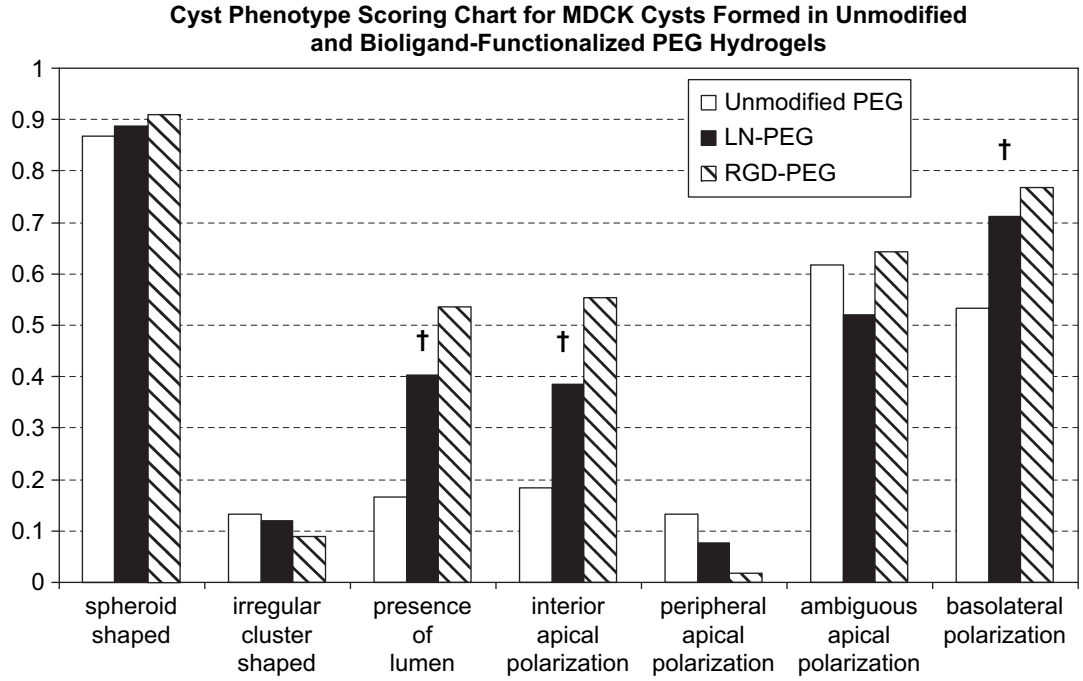

Fig. 6. Scoring chart for the comparison of MDCK cyst phenotypes observed from 15-day 3D cultures in unmodified PEG hydrogels and PEG hydrogels grafted with LN or RGD. Scores of 1.0 being the fullest extent, and have the closest resemblance to the phenotypes of a classical MDCK cyst grown in type I collagen gel; whereas scores of 0 being the opposite. Note that exceptions are for parameters "irregular cluster shaped" and "peripheral apical polarization", which are the phenotypes of abnormal cysts. † Denotes that parameter exhibited significant differences among groups.

previous blocking antibody studies. Activation of β_1 integrin is crucial for the maintenance of normal polarization and function of epithelial tissues; when β_1 integrin-mediated adhesion was disrupted either by the addition of β_1 integrin function-blocking antibodies or by culturing in suspension (i.e. no ECM contact), MDCK cells formed defective cysts with inverted polarity [8,28,39,40]. Similarly, blocking of laminin fragments using monoclonal antibodies indicated that laminin facilitated cell adhesion and selectively promoted epithelial proliferation and polarization [41,42]. Furthermore, addition of excess exogenous laminin rescues the defects in polarization induced by blocking of β_1 integrin [28].

MDCK cysts grown in unfunctionalized PEG gels formed cysts displaying abnormal phenotypes with inverted polarization (apical domain on the outside, basolateral domain on the inside) and missing lumen, similar to the observations with cells grown in suspension [8]. However, some cysts in unmodified PEG gel cultures appeared to have normal polarity (although most of them were without lumen). We attribute this limited differentiation to secretion of laminin at their basolateral surface [26,43–45] that compensates for the lack of an appropriate ECM.

Our results for the 3D MDCK cultures in PEG gels functionalized with bioadhesive motifs demonstrated that these engineered microenvironments promoted epithelial morphogenesis compared to unmodified gels. Interestingly, RGD-functionalized gels promoted higher levels of morphogenesis compared to the LN-tethered gels. This is a surprising observation given LN's critical role in epithelial morphogenesis. The reduced activity of the tethered LN compared to that of RGD could be due to (i) differences in tethered density and/or (ii) structural changes in the tethered LN that reduced biological activity. Future studies in our laboratory will systematically analyze the effects of bioligand density and adhesive activity on epithelial morphogenesis. Finally, these biosynthetic hydrogels could be exploited as engineered matrices to reconstitute the three-dimensional polarized organization and higher order cellular architectures of native epithelial tissues for tissue engineering and regenerative medicine applications.

5. Conclusion

We have engineered proteolytically degradable, bioadhesive PEG hydrogels as a novel 3D model bioartificial matrix that supports epithelial morphogenesis. Epithelial cysts formed in bioadhesive ligand-functionalized PEG gels exhibited a higher frequency of central lumen and interior apical pole formation as well as basolateral polarization compared to those in unmodified PEG hydrogels. These results demonstrate that the incorporation of specific bioadhesive motifs into synthetic hydrogels provides 3D culture environments that support epithelial morphogenesis. These microenvironments provide a flexible and controlled system for systematic investigations into normal and pathologic behaviours as well as bioartificial microenvironments for higher order cellular architectures for regenerative medicine applications.

Acknowledgements

This work was funded by the EPSRC (EP/C535413/1), NIH (R01 EB-004496) and the Georgia Tech/Emory NSF ERC on the Engineering of Living Tissues (EEC-9731643). The authors gratefully acknowledge A. Datta (UCSF) for technical recommendations for 3D culture and analysis, S. Stabenfeldt and M. LaPlaca (Georgia Tech) for helpful suggestions for LN functionalization, and M. Lutolf (EPFL) for hydrogel preparation and cell culture.

References

[1] Schock F, Perrimon N. Molecular mechanisms of epithelial morphogenesis. Annu Rev Cell Biol 2002;18:463–93.
[2] Edelman GM. Cell adhesion molecules in the regulation of animal form and tissue pattern. Annu Rev Cell Biol 1986;2:81–116.
[3] Takeichi M. The cadherins: cell–cell adhesion molecules controlling animal morphogenesis. Development 1988;102:639–55.
[4] Ekblom P, Vestweber D, Kemler R. Cell–matrix interactions and cell adhesion during development. Annu Rev Cell Biol 1986;2:27–47.
[5] Martin GR, Timpl R. Laminin and other basement membrane components. Annu Rev Cell Biol 1987;3:57–85.
[6] Hay ED. Extracellular matrix. New York: Plenum; 1981.
[7] Bernfield M, Banerjee SD, Koda JE, Rapraeger AC. Remodelling of the basement membrane as a mechanism of morphogenetic tissue interaction. In: Trelstad R, editor. Role of extracellular matrix in development. New York: A.R. Liss; 1984.
[8] Wang AZ, Ojakian GK, Nelson WJ. Steps in the morphogenesis of a polarized epithelium. I. Uncoupling the roles of cell–cell and cell–substratum contact in establishing plasma membrane polarity in multicellular epithelial (MDCK) cysts. J Cell Sci 1990;95:137–51.
[9] O'Brien LE, Zegers MM, Mostov KE. Opinion: building epithelial architecture: insights from three-dimensional culture models. Nat Rev Mol Cell Biol 2002;3:531–7.
[10] Leptin M. *Drosophila* gastrulation: from pattern formation to morphogenesis. Annu Rev Cell Dev Biol 1995;11:189–212.
[11] Montell DJ. Command and control: regulatory pathways controlling invasive behavior of the border cells. Mech Dev 2001;105:19–25.
[12] Oda H, Tsukita S. Real-time imaging of cell–cell adherens junctions reveals that *Drosophila* mesoderm invagination begins with two phases of apical constriction of cells. J Cell Sci 2001;114:493–501.
[13] Gumbiner BM. Cell adhesion: the molecular basis of tissue architecture and morphogenesis. Cell 1996;84:345–57.
[14] Conlon I, Raff M. Size control in animal development. Cell 1999;96:235–44.
[15] Vaux DL, Korsmeyer SJ. Cell death in development. Cell 1999;96:245–54.
[16] Alberts B, Bray D, Johnson A, Lewis J, Raff M, Roberts K, et al. Essential cell biology. New York: Garland Publishing; 1998.
[17] Christiansen JJ, Rajasekaran SA, Moy P, Butch A, Goodglick L, Gu Z, et al. Polarity of prostate specific membrane antigen, prostate stem cell antigen, and prostate specific antigen in prostate tissue and in a cultured epithelial cell line. Prostate 2003;55:9–19.
[18] Simons K, Wandinger-Ness A. Polarized sorting in epithelia. Cell 1990;62:207–10.
[19] Gibson MC, Perrimon N. Apicobasal polarization: epithelial form and function. Curr Opin Cell Biol 2003;15:747–52.
[20] Kreitzer G, Schmoranzer J, Low SH, Li X, Gan Y, Weimbs T, et al. Three-dimensional analysis of post-Golgi carrier exocytosis in epithelial cells. Nat Cell Biol 2003;5:126–36.
[21] Hall HG, Farson DA, Bissell MJ. Lumen formation by epithelial cell lines in response to collagen overlay: a morphogenetic model in culture. Proc Natl Acad Sci U S A 1982;79:4672–6.
[22] Hagios C, Lochter A, Bissell MJ. Tissue architecture: the ultimate regulator of epithelial function? Philos Trans R Soc London B Biol Sci 1998;353:857–70.
[23] Weaver VM, Bissell MJ. Functional culture models to study mechanisms governing apoptosis in normal and malignant mammary epithelial cells. J Mammary Gland Biol Neoplasia 1999;4:193–201.
[24] Nelson CM, Bissell MJ. Modeling dynamic reciprocity: engineering three-dimensional culture models of breast architecture, function, and neoplastic transformation. Semin Cancer Biol 2005;15:342–52.
[25] Saxen L. Organogenesis of the kidney. Cambridge University Press; 1987.
[26] O'Brien LE, Jou TS, Pollack AL, Zhang Q, Hansen SH, Yurchenco P, et al. Rac1 orientates epithelial apical polarity through effects on basolateral laminin assembly. Nat Cell Biol 2001;3:831–8.
[27] Pollack AL, Runyan RB, Mostov KE. Morphogenetic mechanisms of epithelial tubulogenesis: MDCK cell polarity is transiently rearranged without loss of cell–cell contact during scatter factor/hepatocyte growth factor-induced tubulogenesis. Dev Biol 1998;204:64–79.
[28] Yu W, Datta A, Leroy P, O'Brien LE, Mak G, Jou TS, et al. Beta1-integrin orients epithelial polarity via rac1 and laminin. Mol Biol Cell 2005;16:433–45.
[29] Abuchowski A, McCoy JR, Palczuk NC, van Es T, Davis FF. Effect of covalent attachment of polyethylene glycol on immunogenicity and circulating life of bovine liver catalase. J Biol Chem 1977;252:3582–6.
[30] Harris JM. Poly(ethylene glycol) chemistry: biotechnical and biomedical applications. New York: Plenum Press; 2000.
[31] Lutolf MP, Raeber GP, Zisch AH, Tirelli N, Hubbell JA. Cell-responsive synthetic hydrogels. Adv Mater 2003;15:888–92.
[32] Raeber GP, Lutolf MP, Hubbell JA. Molecularly engineered PEG hydrogels: a novel model system for proteolytically mediated cell migration. Biophys J 2005;89:1374–88.
[33] Lutolf MP, Hubbell JA. Synthesis and physicochemical characterization of end-linked poly(ethylene glycol)-*co*-peptide hydrogels formed by Michael-type addition. Biomacromolecules 2003;4:713–22.
[34] Nagase H, Fields GB. Human matrix metalloproteinase specificity studies using collagen sequence-based synthetic peptides. Biopolymers 1996;40:399–416.
[35] Hahn MS, Miller JS, West JL. Three dimensional biochemical and biomechanical patterning of hydrogels for guiding cell behaviour. Adv Mater 2006;18:2679–84.
[36] Flory PJ. Principles of polymer chemistry. Ithaca, New York: Cornell University Press; 1953.

[37] West JL, Hubbell JA. Separation of the arterial wall from blood contact using hydrogel barriers reduces intimal thickening after balloon injury in the rat: the roles of medial and luminal factors in arterial healing. Proc Natl Acad Sci U S A 1996;93:13188–93.
[38] Obara M, Yoshizato K. Possible involvement of the interaction of the alpha 5 subunit of alpha 5 beta 1 integrin with the synergistic region of the central cell-binding domain of fibronectin in cells to fibronectin binding. Exp Cell Res 1995;216:273–6.
[39] Klinowska TC, Soriano JV, Edwards GM, Oliver JM, Valentijn AJ, Montesano R, et al. Laminin and beta1 integrins are crucial for normal mammary gland development in the mouse. Dev Biol 1999;215:13–32.
[40] Ojakian GK, Ratcliffe DR, Schwimmer R. Integrin regulation of cell–cell adhesion during epithelial tubule formation. J Cell Sci 2001;114:941–52.
[41] Schuger L, Skubitz AP, de las Morenas A, Gilbride K. Two separate domains of laminin promote lung organogenesis by different mechanisms of action. Dev Biol 1995;169:520–32.
[42] Schuger L, Yurchenco P, Relan NK, Yang Y. Laminin fragment E4 inhibition studies: basement membrane assembly and embryonic lung epithelial cell polarization requires laminin polymerization. Int J Dev Biol 1998;42:217–20.
[43] Henry MD, Campbell KP. A role for dystroglycan in basement membrane assembly. Cell 1998;95:859–70.
[44] Colognato H, Winkelmann DA, Yurchenco PD. Laminin polymerization induces a receptor–cytoskeleton network. J Cell Biol 1999;145:619–31.
[45] Caplan MJ, Stow JL, Newman AP, Madri J, Anderson HC, Farquhar MG, et al. Dependence on pH of polarized sorting of secreted proteins. Nature 1987;329:632–5.